Available online at www.sciencedirect.com

SCIENCE DIRECT®

Biochimica et Biophysica Acta 1556 (2002) 254–264

BIOCHIMICA ET BIOPHYSICA ACTA

BBA

www.bba-direct.com

Stabilization of iron–sulfur cluster F_X by intra-subunit interactions unraveled by suppressor and second site-directed mutations in PsaB of Photosystem I

Ming-Tao Zeng[a,1], Xiao-Min Gong[a,2], Michael C.W. Evans[b], Nathan Nelson[a], Chanoch Carmeli[a,*]

[a] *Department of Biochemistry, Tel Aviv University, Tel Aviv 69978, Israel*

[b] *Department of Biology, University College London, London WC1E 6BT London, UK*

Received 18 July 2002; received in revised form 2 October 2002; accepted 16 October 2002

Abstract

Intra-subunit interactions in the environment of the iron–sulfur cluster F_X in Photosystem I (PS I) of *Synechocystis* sp. PCC 6803 were studied by site-directed and second site suppressor mutations. In subunit PsaB, the cysteine ligand (C565) of F_X and a conserved aspartate (D566) adjacent to C565 were modified. The resulting mutants D566E, C556S/D566E, C556H/D566E and C565H/D566E did not assemble PS I in the thylakoids of the cyanobacterium. Yet, this is the first report of cells of the second site-suppressor mutant (D566E/L416P) and of second site-directed mutant (C565S/D566E) in PsaB that could grow autotrophically in light and were found to assemble a stable functional PS I containing all three iron–sulfur centers, F_X and $F_{A/B}$. The newly resolved structure of PS I (PDB 1JB0) was used to interpret the functional interactions among the amino acid residues. It is suggested that the stability of F_X is supported by a salt bridge formed between D566, which is adjacent to the cysteine ligand C565 of the iron–sulfur cluster located on loop hi, and R703 located at the start of loop jk. Hydrogen bond between R703 and D571 at the start of loop hi further stabilizes the arginine. Lengthening of the side by 1.2 Å chain in mutation D566E caused destabilization of F_X. The extended side-chain was compensated for by the Fe–O, which is 0.3 Å shorter than the Fe–S bond resulting in stabilization of the F_X in the double mutations C565S/D566E. The suppressor mutation D566E/L416P allowed greater freedom for the salt bridge E566-R703, thus relieving the pressure introduced by the D566E replacement and enabling the formation of F_X. F_X and R703 are therefore stabilized through short- and long-range interactions of the inter-helical loops between h–i, j–k and f–g, respectively.

Keywords: Photosystem I; Iron–sulfur cluster; Electron transport; Suppressor mutation; Spectroscopy; Electron paramagnetic resonance

1. Introduction

Photosystem I (PS I) is a transmembranal multisubunit complex located in the thylakoid membranes of chloroplasts and cyanobacteria. It mediates light-induced electron transfer from plastocyanin or cytochrome *c*553 to ferredoxin [1,2]. In cyanobacteria, the complex consists of at least 11 polypeptides, some of which bind light-harvesting chlorophyll molecules. The reaction center core complex is made up of the heterodimeric PsaA and PsaB subunits, containing the primary electron donor P700, which transfers an electron through the sequential carriers A_0, A_1 and F_X. The final acceptors F_A and F_B are located on another subunit, PsaC. P700 is a chlorophyll *a* dimer, which undergoes light-induced charge separation. The electron carriers A_0, A_1, F_X, F_A and F_B represent a monomeric chlorophyll *a*, a phylloquinone and three [4Fe–4S] iron sulfur centers, respectively. The crystalline structure of PS I from *Synechococcus elongatus* resolved to 2.5 Å revealed that 11 transmembranal helices are contributed by each of the heteodimeric core subunits PsaA and PsaB [3]. F_X is located

Abbreviations: PS I, Photosystem I; F_X, F_A and F_B, [4Fe–4S] iron–sulfur clusters; A_1, a phylloquinone; Chl, chlorophyll; DCIP, 2,6-dichlorophynolindophenol; LAHG, light-activated heterotrophic growth

* Corresponding author. Tel.: +972-3-6409826; fax: +972-3-6406834.

E-mail address: ccarmeli@post.tau.ac.il (C. Carmeli).

[1] Present address: Microbiology and Immunology, University of Rochester Medical Center, Rochester, NY 14642, USA.

[2] Present address: Department of Physics, University of California San Diego, La Jolla, CA 92093, USA.

0005-2728/02/$ - see front matter © 2002 Elsevier Science B.V. All rights reserved.
PII: S0005-2728(02)00370-5

in the center of the core heterodimer at the interface of subunit PsaC. F_X is bound to interhelical loops at this interface [3] as was previously predicted by modeling [4,5]. Thus, F_X is positioned as an intermediate carrier between the initial electron mediators A_0 and A_1 and the final electron acceptors of PS I F_A and F_B. Yet, the functional significance of the structural interactions of most of the amino acid side chains and of the iron-cluster ligands is not fully understood.

The midpoint potential of F_X/F_X^- is -705 mV [6], the lowest among the iron–sulfur clusters known in biology. It therefore has the properties required for a carrier that mediates electrons between phylloquinone with redox potential of -800 mV [7] and F_A with -530 mV [8]. Forward electron transfer was shown to proceed through F_X at room temperature by EPR [9,10] and optical spectroscopy [11]. Yet at low temperature, the forward electron transfer to F_X is not kinetically competent [12] since only 13% of the total electron transport proceeds to F_X at 5 K [13] with single turnover flash.

F_X is bound to two inter-helical loops, each belonging to one of the subunits PsaA and PsaB. The X-ray crystal structure indicated that the loop hi connecting α-helices h and i in PsaA/B provides coordinates to F_X [3]. The cysteine residues in the two subunits of the heterodimer, which are in an identical predicted amino acid sequence CDGPGRGGTC [4], bind the iron–sulfur cluster. The two cysteines C556 and C565 that are analogues to C565 and C574 in the crystal structure in PsaB of *Synechocystis* sp. PCC 6803 are the ligands of F_X. Functionally, it was shown that the modification of C556 and C565 to histidine or aspartate resulted in lack of assembly of PS I [14]. Similar results were obtained by modification of an equivalent cysteine to histidine or aspartate in PsaA/B of *Chlamydomonas reinhardtii* [15,16]. Modification of conserved aspartate adjacent to the cysteine and of an arginine in the binding sequence in PsaA/B of *C. reinhardtii* also resulted in a lack of autotrophic growth and, in some cases, PS I could not be assembled [15–17]. The results suggest that a stable F_X was required for proper assembly of PS I. Yet, although the modification of these cysteines to serines in PsaB of *Synechocystis* prevented autotrophic growth, there was an assembly of PS I with decreased capacity for electron transport due to formation of a slightly modified F_X [18].

The interactions of the amino acids in the environment of the cluster can be assumed to contribute to the special redox properties and are expected to be important in the capacity of F_X to stabilize the PS I complex. It is difficult to predict which of the many interactions observed in the structure are essential for function. However, perturbation of the amino acids by mutation can be used to identify the function of these interactions in the environment of F_X in PS I. In this work, we tested such interactions by site-directed mutations in *psaB* in *Synechocystis* sp. PCC 6803. Modification of the cysteine proximal aspartates D557 and D566 to alanine and to lysine in PsaB in *Synechocystis* sp. PCC 6803 only introduced slight instability to PS I [19]. In this study, to our surprise, a milder modification of mutation D566E inhibited the assembly of PS I. Yet, a second site mutation C565S/D566E that recovered PS I assembly gave a clue to the structural role of D566. A preliminary report of these findings was published earlier [20]. It is also the first selection of a mutant in the F_X ligand that can grow photosynthetically. Therefore, analysis of these results was of special significance to the understanding of the function of F_X. The results present additional support to the suggestion that a stable F_X is required for the assembly of PS I. Based on selection of a suppressor mutant, it is suggested that F_X stability is supported by a salt bridge formed between D566, which is adjacent to C565 on loop hi, and R703 located at the start of loop jk. R703 (equivalent to R712 in the crystal structure) that makes the salt bridge is supported by short- and long-range, intra-subunit interactions with side-chain residues in the neighboring loops.

2. Materials and methods

2.1. Directed mutations

Cloning of *psaB* gene and the 3′-end flanking region was done by screening the *Synechosystis* sp. PCC 6803 genomic library with appropriate oligonucleotide probes and identification of the DNA fragments by dot blot and Southern hybridization methods as described [21]. The *psaB* gene and the 0.9 kb 3′ flanking region were amplified by PCR. The PCR products were cloned into pGEM-T Easy vector (Promega) for DNA sequencing by the dye terminator labeling method, with Ready Reaction Cycle Sequencing Kits in ABI PRISM™ 377 DNA Sequencer (Perkin Elmer). For homologous recombination, a clone was constructed on a pBluescript KS vector. The clone contained a 1.8 kb fragment of *psaB* gene and a 1.27 kb *Pst*I fragment of kanamycin resistance-conferring gene from pUC4K [22], ligated downstream to the mutated *psaB* and flanked by the 0.9 kb fragment of the downstream *psaB* flanking region resulting in a pZBL vector (Fig. 1). Oligonucleotide-directed site-specific mutagenesis was performed by overlap extension using PCR [23] with the *psaB* gene as a template.

Amino acid residues proposed to be located in the ligand domain of the iron atoms in the F_X iron–sulfur cluster were changed by site-directed mutagenesis. Replacing aspartate-566 by glutamate (D566E) induced a single mutation in *psaB*, resulting in a unique *Bgl*II restriction site insertion. Double mutation was induced in D566E and in each of the two cysteines of PsaB. Serine or histidine (C556S/D566E, C556H/D566E) replaced C556 and serine or histidine (C565S/D566E, C565H/D566E) replaced C565, respectively. The oligonucleotides used for site-directed mutagenesis of *psaB* are listed in Table 1.

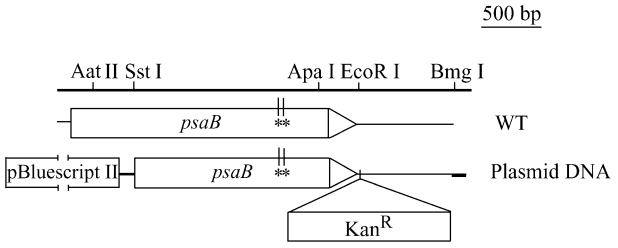

Fig. 1. Scheme for homologous recombination of pZBL vector and the chromosome of wild-type *Synechocystis* sp. PCC 6803. Plasmid pZBL constructed from a pBluescript II KS vector carrying a kanamycin resistance gene (Kan^R) was inserted between the end codon of *psaB* and the flanking region. Mutation sites are indicated by stars next to a unique *Bgl*II restriction site.

2.2. Transformation by homologous recombination of Synechocystis sp. PCC 6803 with the mutated psaB gene

Wild-type *Synechocystis* cells, light-activated heterotrophically grown (LAHG: grown in the dark except for 10 min of light at photon flux density of 40 μmol m^{-2} s^{-1} every 24 h) [24] on BG-11 plates supplemented with 5 mM glucose, 10 mM TES-KOH, pH 8 (*N*-tris[Hydroxymethyl]-methyl-2-aminoethanesulfonate) and thiosulfate (3 g/l), were transformed with the plasmid pZBL cloned with the mutated *psaB* gene. A scheme for homologous recombination is depicted in Fig. 1. The cells were transformed with the resultant plasmids, then selected and segregated for a few generations on 5–20 μg/ml kanamycin. Selection of transformants and segregation were done under kanamycin pressure. Five fully segregated PsaB mutants of *Synechocystis* sp. PCC 6803 were selected. PCR amplification of the genomic DNA of the five PsaB mutants, as well as that of wild type cells, was carried out for evaluation of the segregation and the mutations. Oligonucleotide primers, GTA AAG CTC TCT ATG GCT and GAC AAG CTT AAT TAC CTA ACA G, were used for PCR amplification of a 0.83 kb segment of *psaB* containing the mutated codons and the *Bgl*II restriction site. All of the PCR products were digested to 0.53 and 0.30 kb segments by *Bgl*II in the five PsaB mutants (data not shown). As expected, the PCR product from wild type was not cut by *Bgl*II. DNA sequence analysis confirmed the five mutations of *Synechocystis* sp. PCC 6803 in PsaB.

2.3. Characterization of mutants

Cells of wild type and mutants were grown on BG-11 supplemented with 5 mM glucose and thiosulfate (3 g/l) in the light or under LAHG condition. The harvested cells were washed and broken in a French Pressure Cell and the thylakoids were isolated. PS I was solublilized by detergents (*n*-dodecyl β-D-maltoside) and purified on DEAE-cellulose columns and on sucrose gradient as described [25]. Growth of cells was monitored by measurements of absorption changes at 730 nm. SDS polyacrylamide gel electrophoresis and Western blotting were done as previously described [26,27] and membrane proteins were determined after solubilization in 1% SDS as described [28]. Photosynthetic activity in cells and thylakoids was followed by measuring light-induced oxygen uptake due to the Mehler reaction by an oxygen electrode in the presence of 3 mM methyl viologen as electron acceptor [29]. PS I activity was measured in a reaction mixture containing 50 mM Tris–HCl (pH 8.0), 1.8 μM 2,6-dichlorophenol indophenol (DCPIP), 1 mM sodium ascorbate as electron donor to PS I, 3 mM methyl viologen as an electron acceptor and 0.5 mM of the PS II inhibitor 3-(3,4-dichlorophenyl)-1,1-dimethylurea (DCMU). Chlorophyll concentration and P700 photooxidation were determined according to published methods [30,31]. Flash-induced transient absorption changes in P700 were measured by using a modified flash photolysis setup that included a 10 ns flash from Quantal Nd-YAG laser at 532 nm. A measuring beam was provided by a tungsten-iodide source passed through a monochromator. The absorption changes were monitored by a photomultiplier, interfaced to a Tektronix TDS 520A Digitizing Oscilloscope and recorded on a PC computer. The reaction medium contained 50 mM Tris–HCl, pH 8.0, 1.7 mM sodium ascorbate, 30 μM DCPIP and 50 μg Chl/ml for thylakoids or 30 μg Chl/ml for PS I. Kinetic analysis of the decay of $P700^+$ was done with KaleidaGraph 3.5 program, Synergy Software, Reading, PA. The data were fitted to the multiexponents equation $A_t = A_n e_n^{-kt} + A_{n+1} e_{n+1}^{-kt} \ldots + A_1$ where A_t, A_n, and A_1 are the changes in absorption ampli-

Table 1
Sequences of the oligonucleotides used for site-directed mutagenesis in the *psaB* gene of *Synechocystis* sp. PCC 6803

Mutation sites	Sequences (5′–3′)
C556S/D566E	AAGCAGAGATCTCGCAGGTACCGCCACGGCCGGGGCCATCAGAGGGGAAGGA
C556H/D566E	AAGCAGAGATCTCGCAGGTACCGCCACGGCCGGGGCCATCATGGGGGAAGGA
C565S/D566E	AAGCAGAGATCTCGGAGGTACCGCCACGGCCGGGGCCATCACAGGGGAAGGA
C565H/D566E	AAGCAGAGATCTCGTGGGTACCGCCACGGCCGGGGCCATCACAGGGGAAGGA
D566E	AAGCAGAGATCTCGCAGGTACCGCCACGGCCGGGGCCATCACAGGGGAAGGA
WT[a]	AAGCAGAGATGTCGCAGGTACCGCCACGGCCGGGGCCATCACAGGGGAAGGA

In each case, the introduced mutation site has been underlined.
[a] Wild type corresponding sequence was included in the table for reference.

tude with time (t), the absorption amplitude of the first-order kinetic constants (k_n, k_{n+1}...) and the absorption amplitude that could not be fitted, respectively. Only data with non-linear curve fit statistical values having correlation coefficient of better than 0.94 were used.

2.4. Electron paramagnetic resonance (EPR) spectroscopy measurements

Thylakoid samples were washed with 50 mM Tris–HCl, pH 8.3 containing 5 mM Na-EDTA and 10 mM $MgSO_4$, and finally suspended in 50 mM Tris–HCl, pH 8.3 at 4 °C; PS I complex was dialyzed overnight in 50 mM Tris–HCl, pH 8 at 4 °C, concentrated by Amicon Cell with YM-100 membrane and stored at −80 °C. EPR spectra were recorded on a JEOL RE1X spectrometer fitted with an Oxford Instruments ESR9 liquid helium cryostat.

3. Results

3.1. Site-directed mutations in psaB

The F_X iron–sulfur cluster bridges the PsaA and PsaB polypeptides. The ligands for the irons are two cysteine residues from each of the PS I reaction center polypeptides, PsaA and PsaB. The two cysteine ligands from PsaB of *Synechocystis* are C556 and C565 [3]. It was also reported that the cysteine-proximal aspartate D562 (analogous to D557 in PsaB of *Synechocystis*) in PsaB may play an important role in stabilization of the structure formation of PS I in *C. reinhardtii* [17]. Another cysteine-proximal aspartate D566 in *Synechocystis* was assumed to have a special role because it is conserved in all PsaB subunits in plants, algae and cyanobacteria. We therefore used site-directed mutagenesis in *Synechocystis* to investigate the as yet unexplored role of D566 adjacent to C565 that is unique to PsaB. Possible interactions between the cysteines and the adjacent aspartate were explored by induction of double mutations.

3.2. Transformation by homologous recombination and growth of psaB mutants of Synechocystis

Wild-type *Synechocystis* sp. PCC 6803 cells, grown under LAHG conditions, were transformed with the plasmids cloned with the mutated *psaB* gene. A scheme for homologous recombination is depicted in Fig. 1. Selection of transformants and segregation were done under kanamycin pressure. Five fully segregated PsaB mutants of *Synechocystis* sp. PCC 6803 were selected. There was no significant difference in the growth rates among the five PsaB mutants and the wild type *Synechocystis* grown under LAHG conditions, indicating that functional PS I was not an obligatory condition for *Synechocystis* cells to grow with glucose as a source of carbon. In contrast to the PsaB single mutant C565S of *Synechocystis* that was incapable of autotrophic growth [14], the double mutant C565S/D566E grew autotrophically without glucose under light, but at half the growth rate of the wild type. Mutants C556S/D566E, C556H/D566E, C565H/D566E and D566E could not grow autotrophically in the light without glucose supplement.

3.3. Absorption spectra of wild type and PsaB mutants of Synechocystis sp. PCC 6803

For a more quantitative analysis of the spectral features of these mutant strains, absorption spectra of intact cells were measured. Spectra were corrected for scattering by putting one layer of lens cleaning tissue paper in the reference beam. The absorption spectra of intact cells of wild-type and the mutant strains C565S/D566E and D566E are presented in Fig. 2.

There was an accumulation of chlorophyll in all cells as seen from the absorption maxima at 681 and 438 nm. The amount of chlorophyll per cell was the highest in the wild type, lower in the C565S/D566E mutant and smallest in the D566E mutant. The amount of chlorophyll *a* was also lower in the C565S/D566E mutant than in the wild type. As seen in Fig. 2, the peak of chlorophyll *a* at 685–690 nm in the wild type was decreased and can be seen as a shoulder in the C565S/D566E mutant. The other mutants had spectra similar to the D566E mutant. However, the absorption maximum at 628 nm, originating from phycobilins, was higher in the mutant strains. As a result, the phycobilins/chlorophyll ratio was substantially higher in the mutant strains than in the wild type. This leads to a pronounced "blue" phenotype of the mutant strains. The results could indicate a decreased accumulation of PS I in C565S/D566E or lack of assembly in the other mutant strains.

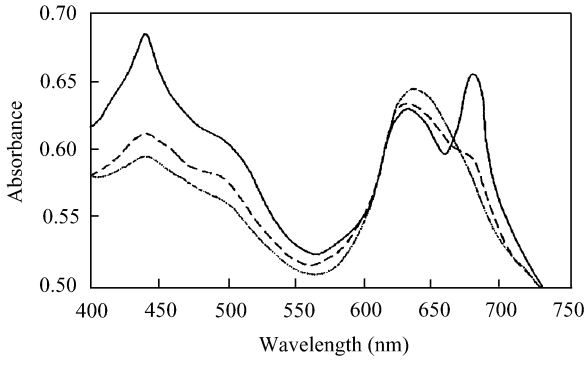

Fig. 2. Absorption spectra of cells of wild type and PsaB C565S/D566E, D566E mutants of *Synechocystis* sp. PCC 6803. In vivo recording of the absorption spectra of whole cells of the wild type (_) and mutant C565S/D566E (- - -) and D566E (·) of *Synechocystis* 6803. The samples were adjusted for equal light scattering at 730 nm (A=0.5). Cells were grown in glucose supplemented BG-11 liquid medium in the light or under LAHG conditions. Samples were taken for spectral measurements during the exponential growth stage. Spectra were corrected for scattering by insertion of one layer of lens cleaning tissue paper in the reference beam.

3.4. Characterization of PS I in thylakoids of wild type and PsaB mutants

Complete absence or a low rate of photosynthetic growth in the mutants could be a result of either deficient assembly of the photosynthetic apparatus or its impaired activity. It was therefore necessary to measure the components of the photosynthetic systems and their activity. Chlorophyll accumulation in *Synechocystis* reflects the accumulation of photosynthetic reaction center proteins. The ratio of chlorophyll to protein was lower in the thylakoids of mutants than in that of the wild type, probably because less photosynthetic components were assembled in the mutants (Table 2). Subunits PsaA/PsaB of wild type PS I appeared as diffuse 55–70 kDa bands in SDS-PAGE. The attempts to show the presence of the PsaA/PsaB heterodimer in PS I preparations of mutants D566E, C556S/D566E, C556H/D566E and C565H/D566E by SDS-PAGE analysis failed, thus indicating a low level of assembly of PsaA/PsaB in these mutants (data not shown).

PS I activity was measured by light-induced oxygen uptake. The reaction mixture contained 20 μg Chl/ml, 50 mM Tris–HCl (pH 8.0) and 1.8 μM DCPIP, 1.0 mM sodium ascorbate, 3 mM methyl viologen and 0.5 mM DCMU. Oxygen uptake was determined with a Hansatech electrode at 30°. Net rates of light-induced oxygen uptake were obtained by subtraction of the rates measured after light was turned off. For protein assay, samples were hydrolyzed with 0.5 N NaOH and determined using BSA as protein standard. Ratio of chlorophyll to protein was calculated as wt/wt.

To assay more precisely the accumulation of the PsaA/PsaB heterodimer in PS I, immunoblotting of the thylakoids was performed with antibody against PsaA/PsaB (Fig. 3). The amount of protein from C565S/D566E appeared to be approximately 60% of that of wild type, while the cross reaction of the antibody to proteins from D566E, C556S/D566E, C556H/D566E and C556H/D566E is hardly detectable. It was earlier shown that site-directed mutations in *psaB* did not prevent the expression of the gene. It is suggested that the mutant cells are capable of expressing mutated *psaB* but the gene products are unable to form a correct F_X structure; therefore, the breakdown of the gene products is higher than in the wild type. This is especially significant in mutants D566E, C556S/D566E, C556H/D566E and C556H/D566E.

Table 2
Photosystem I activity and ratio of chlorophyll to protein in thylakoids of wild type and PsaB mutants of *Synechocystis* sp. PCC 6803

Strains	O_2 uptake (μmol O_2/mg Chl/h)	Chl/protein (mg/mg × 10^{-3})
WT	125	9.9
C565S/D566E	82	7.9
C556S/D566E	3	7.0
C556H/D566E	2	6.0
C565H/D566E	2	6.8
D566E	3	7.4
D566E/L416P	124	9.8

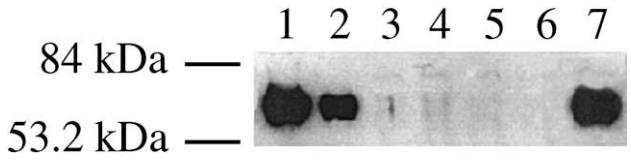

Fig. 3. Immunochemical detection of PsaA/PsaB polypeptides of the PS I complex. Thylakoid samples containing 5 μg chl were applied to each lane. After SDS-PAGE, proteins were transferred from the gel to nitrocellulose membrane. Relative molecular weights were estimated by comparison with prestained molecular size standards (Bio-Rad Laboratories, CA). Immunoblots were incubated in blocking solution overnight at 4 °C, then incubated with the primary antibody recognizing PsaA/PsaB and the secondary antibody-goat anti-rabbit IgG conjugated to horseradish peroxidase (Sigma Israel). The detection reaction was performed by a modified ECL method (Amersham). Lanes 1, 2, 3, 4, 5, 6 and 7 are thylakoids from wild type, C556S/D566E, C556H/D566E, C565S/D566E, D566E, C565H/D566E and D566/L416P, respectively.

PS I activity was measured by the determination of the light-induced electron transport rate, in the presence of ascorbate reduced DCIP as an electron donor and methyl viologen as an electron acceptor of PS I and DCMU as an inhibitor of PS II. The rate of oxygen uptake by isolated thylakoids of mutant C565S/D566E was 2/3 of wild-type thylakoids. The rates of oxygen uptake by isolated thylakoids of mutants C556S/D566E, C556H/D566E, C565H/D566E and D566E were all approximately the same and very low compared to the rate in wild type (Table 2). The reduced rates of oxygen uptake measured in thylakoids of mutants C556S/D566E, C556H/D566E, C565H/D566E and D566E are likely to be the result of the lack of assembly of PS I.

3.5. Kinetic analysis of P700 reversible photooxidation in PS I of wild type and PsaB mutants

The function of PS I in PsaB mutant at physiological temperature was determined by measurement of the reversible photooxidation and flash induced transient absorption changes of P700. Photobleaching of P700 under continuous illumination gave a molar ratio of chlorophyll to P700 of 101 and 147 for PS I isolated from autotrophically grown cells of the wild type and of the C565S/D566E mutant strains, respectively. The faster rate of reduction following the oxidation of P700 by single turnover flash observed in the mutant PS I (Fig. 5) could cause an apparent lower oxidation level at steady state illumination and result in a higher chlorophyll to P700 ratio.

Spectral overlap of F_X, $F_{A/B}$ and P700 at 430 nm interferes with direct determination of electron transfer to F_X. However, the recombination of the intermediate carriers with $P700^+$ can be determined from the rate of decay of $P700^+$. The time constants derived from the kinetic transients of P700 measured at 700 nm and 820 nm were used to

identify the relative contributions of various electron acceptors to $P700^+$. The lifetime values of the back electron transfer from different components of the PS I acceptor side of $P700^+$ are 10 ns (A_o); 10–110 μs (A_1); 400–1.5 ms (F_x); and 10–100 ms ($F_{A/B}$) [2].

The kinetics of light-induced absorption changes, A_{820}, of wild-type thylakoids was resolved into two components. The half-lives ($t_{1/2}$) were 19.5 ± 5 ms for 37.4% of the total absorption change and 121.3 ± 35 ms for 53% of the absorption change for the faster and slower components, respectively. The rest 9.6% of the absorption decayed in a slower unresolved decay component. In thylakoids isolated from the mutant C565S/D566E, the $t_{1/2}$ values were 18 ± 2 ms (42%) and 168 ± 20 ms (58%), respectively (Fig. 4a,b). The $t_{1/2}$ of 19.5 ± 5 ms of the decay in the wild-type thylakoids was assigned mostly to $P700^+/F_{A/B}^-$ recombination. The decay kinetics of $t_{1/2}$ of 121.3 ± 35 ms might be partially due to a slow component of $P700^+/F_{A/B}^-$ recombination. Part of it as well as the additional kinetically undetermined 9.6% of the absorption might be a result of reduction of $P700^+$ by DCIP replacing the electrons that escaped from PS I to an unidentified electron acceptor.

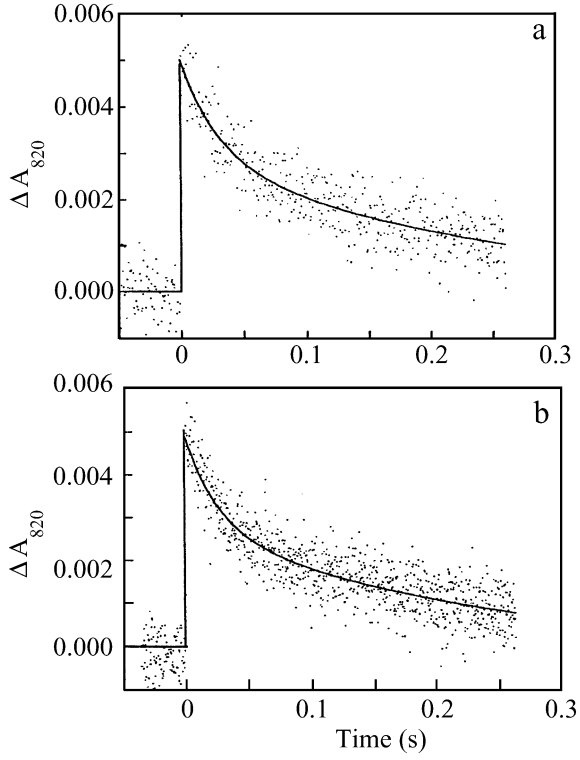

Fig. 4. Flash-induced transient absorption changes of P700 in thylakoids of wild type and C565S/D566E mutant of *Synechocystis* sp. PCC 6803. The absorption changes of P700 were monitored at 820 nm (A_{820}) following a saturating laser flash in wild type (a) and in C565S/D566E mutant (b) thylakoids. The measurements were performed with 50 μg/ml chlorophyll in 50 mM Tris–HCl, pH 8.0, containing 30 μM DCPIP and 1.7 mM sodium ascorbate. The samples were incubated in darkness before a saturating flash was applied at 22 °C. Thylakoids were prepared from cells grown under mixotrophic conditions.

Faster decay kinetics was observed in the mutant C565S/D566E. The absorption change, with $t_{1/2}$ of 18 ± 2 ms (42%), was a result of two unresolved kinetic phases that appear as one phase. This suggestion is based on the finding that in the isolated PS I of the C565S/D566E mutant, the analysis of the data that have higher signal to noise ratio indicated an additional component of the decay that was resolved to 3.8 ms (10%). It might have been consisted of a contribution from the recombination of $P700^+/F_X^-$ and of the fast component of the recombination of $P700^+/F_{A/B}^-$. The remaining 58% of the decay was contributed by a slow component of $P700^+/F_{A/B}^-$ recombination and the reduction was due to the depletion of electrons that reduced an unidentified oxidant. It is possible that in mutant C565S/D566E, a change in the redox potential of the F_X or a change in the rate of forward electron transfer caused a faster back reaction to $P700^+$. These results were further verified by measuring the ΔA_{820} decay in PS I complexes isolated from wild type and mutant C565S/D566E cells.

Essentially similar results were obtained when the decay of P700 oxidation was measured at 820 nm in isolated PS I. The wild type PS I complex also showed multiple decay kinetics. A decay with $t_{1/2}$ values of 36 ± 4 ms (37%), and 92 ± 10 ms (38%) was ascribed to a back reaction from $F_{A/B}^-$. The decay with $t_{1/2}$ of >92 ms (25%) was due to the back reaction from DCIP (Fig. 5a). The kinetics of the mutant C565S/D566E PS I complex was considerably different from the kinetics of the wild type (Fig. 5b). There were 3.8 ± 0.4 ms (10%), 48 ± 5 ms (41%) and >48 ms (49%). The slower kinetic components were attributed to a back reaction from $F_{A/B}^-$ and reduction of $P700^+$ by DCIP that compensated for the electrons that escaped from PS I due to the oxidation of $F_{A/B}^-$ by an unknown acceptor. The faster component in the PS I complex of mutant C565S/D566E indicated some back reaction from the F_X iron–sulfur cluster. In order to resolve the differences in the decay rates, the absorption changes were measured at a faster time scale. As seen in the inset of Fig. 5b, 35% of the absorption change in mutant C565S/D566E decayed at $t_{1/2}$ of 80 ± 12 μs compared to only 20% in the wild type PS I. The decay was attributed partially to back reaction from A_1^- and a decay from chlorophyll triplet. Since 90% of the electrons proceed to $F_{A/B}$, the inefficient growth might be due to a slow down in the forward electron transport to F_X or to PS II-poisoning due to relative low ratio of PS I to PS II.

3.6. EPR spectroscopy analysis of iron–sulfur clusters in thylakoids and PS I complexes from wild type and mutants

EPR spectroscopy was used for direct identification of the terminal iron–sulfur clusters in membranes and in PS I that was isolated from wild type and mutants thylakoids. The light-induced EPR spectra of thylakoids and PS I complexes of the wild types were measured (Fig. 6) in order to compare them with that of the mutants. The iron–sulfur centers of F_A and F_B were reduced by illumination in

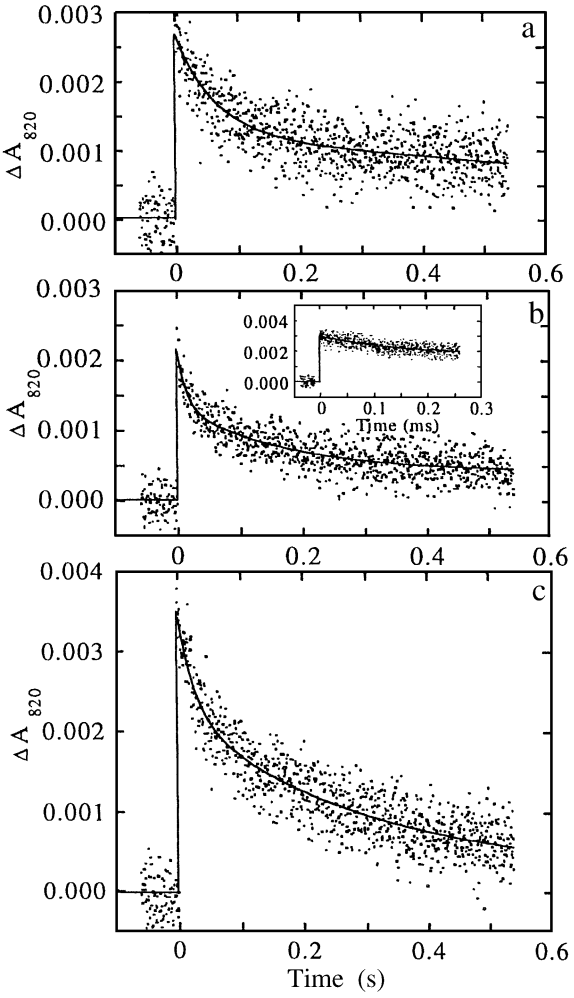

Fig. 5. Flash-induced transient absorption changes of P700 in PS I complexes of wild type, suppressor and C565S/D566E mutant. The absorption changes of P700 were monitored at 820 nm (A_{820}) following a saturating laser flash in wild type (a) and in C565S/D566E mutant (b) and D566E/L416P suppressor mutant (c) PS I complexes. The absorption changes in C565S/D566E mutant were also measured at a microsecond time scale (b, inset). The experiments were performed with 30 μg/ml chlorophyll in 50 mM Tris–HCl, pH 8.0, containing 30 μM DCPIP and 1.7 mM sodium ascorbate. The samples were incubated in the dark before a saturating flash was applied at 22 °C. PS I complex was prepared from cells grown under mixotrophic conditions.

the presence of ascorbate at 15 K. The signals of reduced iron–sulfur centers of F_A and F_B in the thylakoids from the wild type cells (Fig. 6, 1) are similar to those in the isolated PS I complex (Fig. 6, 2), suggesting no major changes on isolation. There was no light-induced signal in the D566E mutant (Fig. 6, 3). Indeed, the presence of PS I and the associated iron–sulfur cluster would not be expected in thylakoids lacking PsaB subunit as was shown by the immunoblot (Fig. 3). Light-induced signal was not observed in the other C556S/D566E, C556H/D566E, or C565H/D566E mutants that did not assemble PS I. The results observed with preparations of the mutant C565S/D566E (Fig. 7) were essentially similar to those seen in the wild type. These results indicated that the terminal clusters $F_{A/B}$ were not modified and could be reduced by light in the mutated PS I. It is unlikely that $F_{A/B}$ could be reduced in the light in the absence of functional F_X in the mutant. It was assumed therefore that the EPR spectrum of the functional F_X in mutant C565S/D566E might be only slightly modified as was earlier observed in the single mutant C565S [18]. Reduction of wild-type thylakoid or of the isolated PS I with sodium dithionite results in the reduction of the F_A and F_B iron–sulfur centers with the typical interaction signals in the EPR spectrum (Fig. 8). The thylakoids from mutant D566E did not show the $F_{A/B}$ iron–sulfur centers, but reduction with dithionite resulted in the appearance of a Fe–S type signal around $g=1.92$. The thylakoids of mutant D566E did not assemble PS I. It is therefore suggested that the EPR signal might belong to a component of the respiratory system as it resembled a signal that we have also seen in preparations of *Phormidium laminosum* [32]. This signal, which was also present in the mutant C565S/D566E preparations, slightly distorted the normal F_A and F_B Fe–S signals in the $g=1.92$ region.

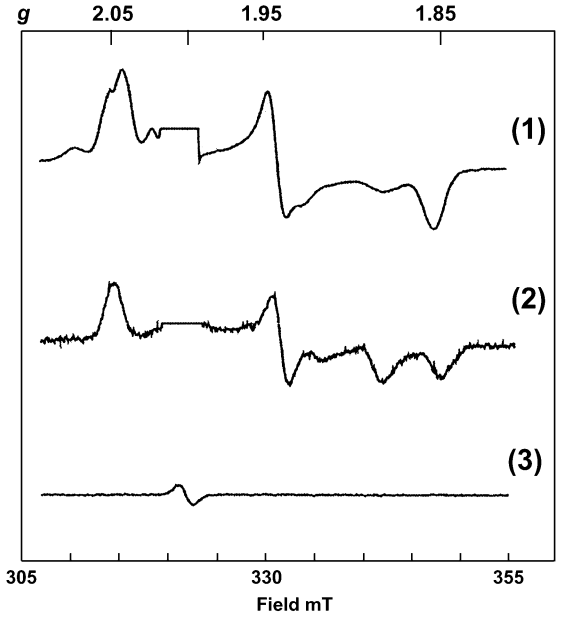

Fig. 6. Light-induced EPR spectra in the $g=2.00$ region of thylakoids and PS I complex from wild type and D566E mutant of *Synechocystis* sp. PCC 6803. The samples in 50 mM Tris buffer, pH 9.0, were reduced with 10 mM sodium ascorbate for 30 min in the dark and then frozen in the dark. Samples were illuminated for 30 s in the spectrometer cavity at 15 K and the spectra were recorded after the light was turned off. The recordings shown are light minus dark difference spectra of samples containing: (1) thylakoids of wild type; (2) PS I complex of wild type and (3) thylakoids of D566E mutant. The signals of the radical in the spectra were assigned as follows: F_A: $g=2.05$, 1.94 and 1.86; F_B: $g=2.05$, 1.93 and 1.88; $P700^+$: $g=2.002$. The large radical at $g=2.002$ of $P700^+$ has been deleted for clarity. EPR measurements were made at 15 K, microwave power 10 mW, modulation width 1 mT and a frequency of 9.055 GHz. The spectra were normalized to show relative intensities for equivalent chlorophyll concentrations.

3.7. Analysis of suppressor mutations selected from site-directed mutants of PsaB in Synechocystis

Most site-directed mutations introduced in this study affected the assembly of the PS I reaction center in the mutants of *Synechocystis* sp. PCC 6803. It was therefore helpful to use suppressor or pseudorevertant mutants to obtain a modified, assembled complex for exploration of the structural and functional relation of the F_X iron–sulfur cluster of PS I. Suppressor or revertant mutant selection was performed under autotrophic growth conditions. PsaB mutant cells were grown to exponential stage, some of them treated with methanesulfonate ethyl ester, and transferred to BG-11 plates. Suppressor or revertant mutants that were selected from autotrophically grown cells were segregated for several generations. Genomic DNA was isolated from cells of each of the suppressor or revertant mutants and *psaB* was amplified by PCR. The amplified fragments of the gene were cloned and sequenced. Four D566E underwent suppression by replacing L416 with proline, forming the same PsaB double mutants D566E/L416P of *Synechocystis* sp. PCC 6803. The cells of the D566E/L416P suppressor mutant were similar to the wild type in autotrophic growth rate, the absorption spectra, the composition and the amount of PS I polypeptides (Fig. 3, lane 7). The rate of electron transport from reduced DCIP to oxygen catalyzed by PS I and the chlorophyll protein ratio were also similar to that which was found in the wild type (Table 2). The $P700^+$ decay measured at 820 nm in PS I complex showed $t_{1/2}$ values of 18.8 ± 2 ms (35%), and 189 ± 18 ms (57%) and was ascribed to a back reaction from

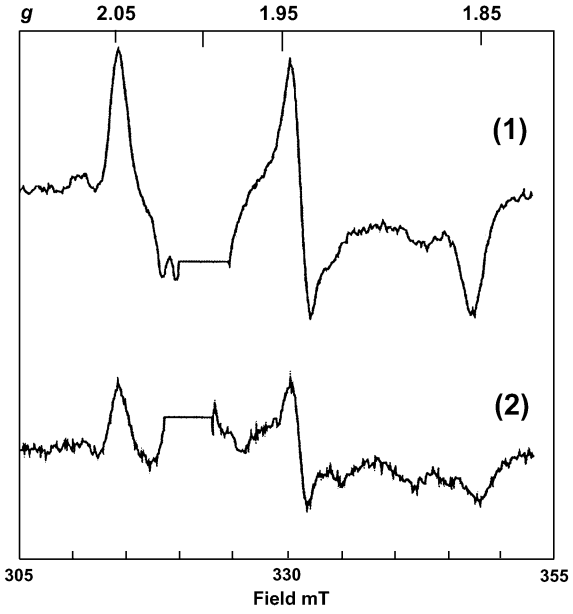

Fig. 7. Light-induced EPR spectra in the $g = 2.00$ region of thylakoids and PS I complex from mutant C565S/D566E of *Synechocystis* sp. PCC 6803. The recordings shown are light minus dark difference spectra of samples containing: (1) thylakoids, and (2) PS I complex. Samples were prepared, spectra were recorded and the signal of radicals in the spectra were assigned to g values as described in Fig. 6.

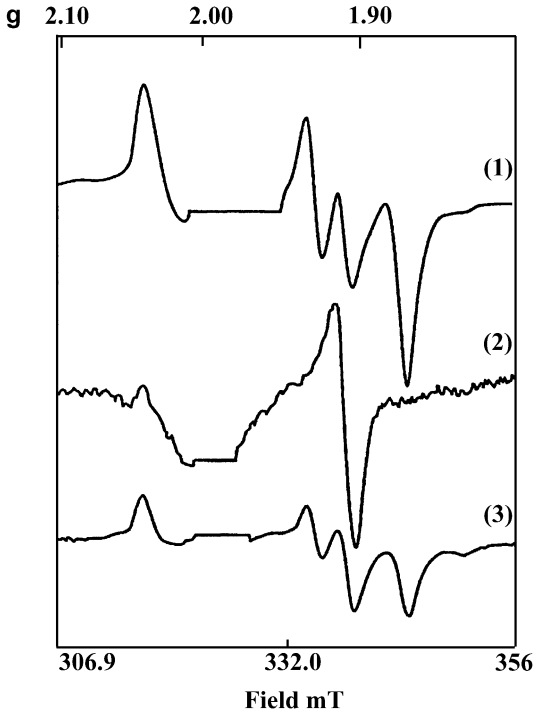

Fig. 8. EPR spectra in the $g = 2.00$ region of chemically reduced thylakoids from wild type and mutants of *Synechocystis* sp. PCC 6803. The thylakoid samples, in 0.2 M glycine-KOH buffer, pH 10, were reduced for 30 min in the dark with 0.2% sodium dithioinite, and frozen in the dark. Spectra of thylakoids from wild type (1), mutant D566E (2) and mutant C565S/D566E (3) were recorded as described in Fig. 6. The g values for centers $F_{A/B}$ were similar to those indicated in Fig. 6. The signal at $g = 1.92$ in D566E is due to a respiratory iron–sulfur center.

$F_{A/B}^-$. The kinetically unresolved decay with $t_{1/2}$ of >190 ms (8%) was due to the back reaction from DCIP (Fig. 5c). Based on hydropathy analysis and the crystallography of PS I, PsaB consists of 11 trans-membrane helices [3,4]. The two mutated cysteine residues (C556 and C565), providing ligands to the F_X iron–sulfur cluster and the adjacent D566, are located on the loop hi between helices h and i (nomenclature according to Ref. [3]). However, in the suppressor mutants, the alterations happened in helix g, some 150 amino acids away from the primary mutation, allowing P416 to be exposed on the surface of the membrane in the loop fg. It is suggested that the suppressor mutation L416P caused a rearrangement of α-helix g, since the cyclic structure of proline is known to break α-helix. This resulted in a new structure. This mutation indicated some short- and long-distance intrasubunit interactions between loops fg, hi and jk.

4. Discussion

4.1. Second site mutations changed protein conformation and enabled the formation of functional PS I

This study reports for the first time the second site suppressor mutation in PsaB, which changed the conforma-

tion of the inactive PS I core protein and enabled assembly of the functional PS I. Analysis of the suppressor mutation facilitated the exploration of the structure–function relationship in the protein.

The perturbation of proteins by site-directed mutations is a powerful tool in the study of the structure function relationship. Yet all site-directed mutations introduced into the ligands of the iron–sulfur cluster F_X failed to produce alterations that could support autotrophic growth of the bacteria or algae [14–17]. Although valuable information was derived from those modifications which could assemble modified PS I under heterotrophic growth, the C565S/D566E double mutant represents the first case in which a modified ligand of F_X could support autotrophic growth. Essential information about the factors that contribute to efficient function of the F_X cluster can be drawn from the differences between this and other mutants, which do not grow photosynthetically. The finding that a second site mutation makes a marked difference underscores the functional importance of intra-subunit structural interactions.

Each of the subunits PsaA and PsaB contain 11 transmembrane helices (labeled a–g) of predominantly hydrophobic amino acid residues interconnected by loops and surface helices containing charged amino acids [3]. The cysteine residues C556 and C565 on loop hi provide two of the four ligands that bind the F_X iron–sulfur cluster. Site-directed mutation of aspartate to glutamate prevented the formation of a stable F_X in the D566E mutant. A change by one carbon increases the side chain of the amino acid by only 1.2 Å. It was previously suggested by us [20] that such a small change could inactivate PS I if the carboxyl of D566 forms a salt bridge with a positively charged amino acid that is in relatively rigid conformation. From the coordinates of the crystalline structure of PS I from *S. elongatus* (Fig. 9), it can be seen that the structure of the iron–sulfur cluster F_X is supported by a salt bridge between D566 and R703 (the equivalents to D575 and R712 in the crystalline structure). This structure can be used for interpretation of the data since there is more than 90% homology between the sequence of PsaA/B of the *Synechococcus* and *Synechocystis*. The rigidity of the salt bridge is due to short-range intra-subunit interactions between D566 on loop (hi) and R703 at the start of the loop (jk), which is further stabilized by forming H-bond to D571 on loop (hi).

Suppressor mutation D566E/L416P indicated the presence of long-range interactions that might stabilize F_X. The interaction spans over 19 Å between D566 and the rigid K413 located just at the end of the trans-membrane helix (g). It can be speculated that one such chain of interaction could consist of salt bridges and H-bonds from D566-R703-D571-S568-I567-K547-HOH163-E537 to K413 that are located on loops hi, jk and fg. We suggest that the suppressor mutation D566E/L416P caused a rearrangement of α-helix g, since the cyclic structure of proline is known to break the α-helix and markedly influence protein architecture. This would result in a new structure that allows P416 to be exposed to the surface of the membrane. Thus, the suppressor mutation breaks the end of helix g and extends loop (fg), rendering more flexibility to K413 at the end of the long-distance interactions. This flexibility makes room for the formation of F_X in mutant D566E/L416P. This chain could represent the long-distance interaction but it is possible that it is not the only or the most effective one that stabilizes F_X. Rigorous optimization and other experimental verifications that are beyond the scope of this work are required to verify this suggestion.

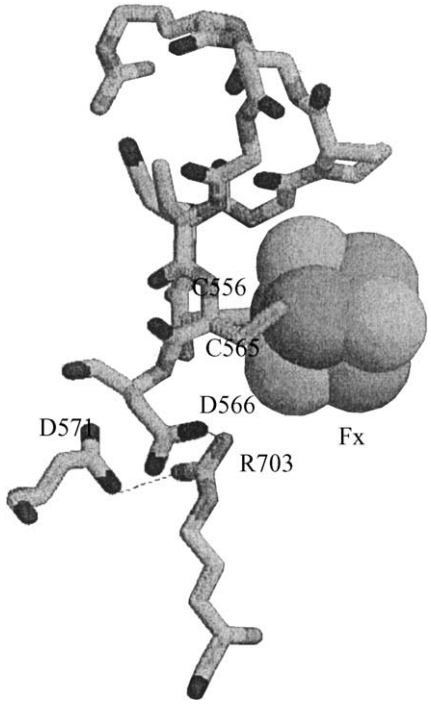

Fig. 9. The iron–sulfur cluster F_X and its protein environment in subunit PsaB. The atoms in the conserved binding sequence of the iron–sulfur cluster on PsaB CDGPGRGGTCD are presented as sticks and the atoms in F_X as space fill models. C556 and C565 are ligands of the irons in the cluster while R703 is shown to form a salt bridge with D566 and a hydrogen bond with D571 (dashed line). The image was created by RasMole 2.6 using the coordinates from PDB 1JBO.

Breaking of the salt bridge between D566 and R703, by introduction of a neutral residue in mutant D566A or a positively charged residue as in the D566K mutations was shown to slightly modify the properties of F_X [19]. The changes were attributed to structural instability but did not cause disintegration of PS I. These findings support our suggestion that the cysteine-proximal aspartate salt bridge is primarily important in maintaining the structural integrity of the iron–sulfur cluster. It can be seen from the structure that R703 that forms a salt bridge with D566 is also H-bonded to D571 (Fig. 9). It is also seen that the distance between D566 and D571 is 4.1 Å. Therefore, in mutation D566K, the K566 can form an H-bond with D571 replacing the salt bridge between D566 and R703 that stabilizes F_X in the wild type. Thus, D571 stabilizes F_X both in the wild type and in mutant D566K. The negatively charged side chain of

aspartate is either too far from the iron to affect the properties of the cluster, or it does not affect it because it is neutralized by the cation making the salt bridge. The importance of cysteine-proximal aspartate to the structure–function integrity of the cluster is also seen from the D576L mutation in PasA of *C. reinhardtii*. The lack of autotrophic growth seems to be a result of a slowdown in electron transfer from the quinone A_1 to F_X. A suppressor mutation of unknown nature accelerated electron transfer to a normal rate and enabled photosynthetic growth [33].

4.2. Structure–function relationship of the F_X iron–sulfur cluster in PS I

The iron–sulfur cluster F_X serves as a unique electron acceptor in PS I. Yet, the mode of electron transfer by this cluster in PS I is not fully resolved. Site-directed mutations targeted to the F_X binding domain in this study provide an insight into the biogenesis, structure and function of the F_X iron–sulfur cluster in the PS I. As shown in the mutants D566E, C556S/D566E, C556H/D566E and C565H/D566E, deficiency in F_X formation directly affected the accumulation of functional PS I. Yet the single mutations C556S and C565S, which could not support photoautotrophic growth, accumulated functional PS I when grown under heterotrophic conditions [15]. This evidence indicates that the iron–sulfur cluster F_X plays a central role in the function as well as in the architecture of PS I.

The specific double mutations C565S/D566E resulted in the assembly of PS I. As suggested, the suppressor mutation D566E/L416P allowed greater freedom for the salt bridge E566 and R703, thus relieving the pressure introduced by D566E replacement and enabling the formation of F_X. The double mutation C565S/D566E enabled the formation of a more stable F_X for similar reasons. Lengthening of the side chain of E566 by 1.2 Å, which caused destabilization, was compensated for by the Fe–O, which is 0.3 Å shorter than the Fe–S bond which stabilizes the F_X. Preliminary analysis of X-ray absorption measurements of the iron in the PS I core preparation of the C565S/D566E mutant indicated that the Fe–O in the cluster is 1.96 Å, compared to the Fe–S distance of 2.26 Å. This suggestion is supported by the finding that shortening of the Fe–S distance in a cysteine ligand of the cluster, some nine amino acids away from E566 in the mutation C556S/D566E, did not reconstitute the lost activity. Replacement of cysteine by the bulkier histidine in mutants C556H/D566E and C565H/D566E also did not reconstitute the lost activity. It can also be suggested that the extended arm of the carboxylate residue in the D566E gave additional structure–function stability to the cluster in the C565S/D566E mutant compared to that of the C565S mutant. The double mutant C565S/D566E was superior to the C565S mutant and enabled photoautotrophic growth.

A mutation in PsaB that did not prevent the assembly of PS I required proper folding and formation of a stable association among the subunits. Either incorrect folding of PsaB or instability in the structure of F_X or instability in subunit interactions could have prevented the assembly of PS I in mutation D566E. Incorrect folding prior to its assembly could have caused digestion of PsaB by proteinases. Incorrect folding was, however, prevented in the double mutant C565S/D566E. The rather conservative mutation C565S did not cause changes in folding of subunit PsaB and allowed the assembly of PS I. Therefore, mutation C565S would not be expected to remedy changes in folding that might have resulted from mutation D566E. It is therefore more likely that the double mutation C565S/D566E resulted in formation of a more stable PS I.

4.3. Mixed-ligand F_X iron–sulfur cluster can mediate electron transfer in PS I

F_X might exist in mutant C565S/D566E as a mixed-ligand cluster in which one cysteine sulfur ligand of the F_x cluster was replaced by serine oxygen. Preliminary results of the X-ray absorption measurements indicated that mixed-ligand iron–sulfur cluster is present in PS I core preparation. There are other known instances where mixed-ligand [4Fe–4S] was generated by site-directed mutagenesis in PS I of *Synechocystis* sp. PCC 6803 [18,34]. Targeted single mutations of C14S, C51S in PsaC and C565S and C556S in PsaB resulted in the formation of a mixed-ligand [4Fe–4S], where one cysteine sulfur was replaced by serine oxygen. The mixed ligand clusters were shown to function in electron transfer in PS I. Although the structures of the mixed-ligand [4Fe–4S] was not determined, the EPR spectra at $g=2$ region of the mixed-ligand F_A and F_B were undetectable, probably because of a change in spin state [34]. There were, however, only small differences between the EPR spectrum of the wild type and the mutant of F_X at the $g=2$ region. These differences were ascribed to the change of one of the iron ligands from sulfur to oxygen [18]. On the basis of the experimental data shown in this study, the three-dimensional structures of the [4Fe–4S] F_X clusters of wild type and mutant C565S/D566E of *Synechocystis* sp. PCC 6803 may be similar to the [4Fe–4S] clusters of ferredoxin. The mixed-ligand cluster F_X was functional but the electron transfer in PS I was modified. Based on preliminary measurements, it is suggested that the modified F_X was less efficient in transferring electron from the quinone A_1 to $F_{A/B}$ in PS I. This led to a significant decrease of electron transfer efficiency in PS I.

References

[1] P.R. Chitnis, N. Nelson, Photosystem I, in: L. Bogoras, I.K. Vsil (Eds.), Photosynthetic Apparatus: Molecular Biology and Operation, Academic Press, New York, 1991, pp. 177–224.
[2] J.H. Golbeck, D.A. Bryant, Curr. Top. Bioenerg. 16 (1991) 83–177.
[3] P. Jordan, P. Fromme, H.T. Witt, O. Klukas, W. Saenger, N. Krauss, Nature 411 (2001) 909–917.
[4] L.E. Fish, U. Kuck, L. Bogorad, J. Biol. Chem. 260 (1985) 1413–1421.

[5] B.D. Bruce, R. Malkin, J. Biol. Chem. 263 (1988) 7302–7308.
[6] M.C.W. Evans, S.G. Reeves, R. Cammack, FEBS Lett. 49 (1974) 111–114.
[7] P. Setif, H. Bottin, Biochemistry 28 (1989) 2689–2697.
[8] M.C.W. Evans, P. Heathcote, Biochim. Biophys. Acta 590 (1980) 89–96.
[9] P. Moenne-Loccoz, P. Heathcote, D.J. Maclachlan, M.C. Berry, I.H. Davis, M.C.W. Evans, Biochemistry 33 (1994) 10037–10042.
[10] A. van der Est, C. Bock, J.H. Golbeck, K. Brettel, P.Q. Setif, D. Stehlik, Biochemistry 33 (1994) 11789–11797.
[11] K. Sigfridsson, O. Hansson, P. Brzezinski, Proc. Natl. Acad. Sci. U. S. A. 90 (1995) 3458–3462.
[12] M.S. Crowder, A.J. Bearden, Biochem. Biophys. Res. Commun. 722 (1983) 23–35.
[13] E. Schlodder, K. Falkenberg, M. Gergeleit, K. Brettel, Biochemistry 37 (1998) 9466–9476.
[14] L.B. Smart, P.V. Warren, J.H. Golbeck, L. McIntosh, Proc. Natl. Acad. Sci. U. S. A. 90 (1993) 1132–1136.
[15] A.N. Webber, P.B. Gibbs, J.B. Ward, S.E. Bingham, J. Biol. Chem. 268 (1997) 12990–12995.
[16] B.J. Hallahan, S. Purton, A. Ivison, D. Wright, M.C.W. Evans, Photosynth. Res. 46 (1995) 257–264.
[17] S.M. Rodday, A.N. Webber, S.E. Bingham, J. Biggins, Biochemistry 34 (1995) 6328–6334.
[18] I.R. Vassiliev, Y.S. Jung, L.B. Smart, R. Schulz, L. McIntosh, J.H. Golbeck, Biophys. J. 69 (1995) 1544–1553.
[19] I.R. Vassiliev, J. Yu, Y.S. Jung, R. Schulz, A.O. Ganago, L. McIntosh, J.H. Golbeck, J. Biol. Chem. 274 (1999) 9993–10001.
[20] M. Zeng, I. Sagi, M.C.W. Evans, N. Nelson, C. Carmeli, in: G. Gabar, J. Pusztai (Eds.), Photosynthesis: Mechanisms and Effects, Kluwer Academic Publishing, Dordrecht, 1999, pp. 643–646.
[21] P.R. Chitnis, D. Purvis, N. Nelson, J. Biol. Chem. 266 (1991) 20146–20151.
[22] J. Vieira, J. Messing, Gene 19 (1982) 259–268.
[23] S.N. Ho, H.D. Hunt, R.M. Horton, J.K. Pullen, L.R. Pease, Gene 77 (1989) 51–59.
[24] S.L. Anderson, L. McIntosh, J. Bacteriol. 173 (1991) 2761–2767.
[25] R. Nechushtai, P. Muster, A. Binder, V. Liveanu, N. Nelson, Proc. Natl. Acad. Sci. U. S. A. 80 (1983) 1179–1183.
[26] U.K. Laemmli, Nature 227 (1970) 680–685.
[27] N. Nelson, Methods Enzymol. 118 (1986) 352–369.
[28] O.H. Lowry, N.L. Rosenbrough, A.L. Farr, R.J. Randall, J. Biol. Chem. 193 (1951) 265–275.
[29] S. Izawa, Methods Enzymol. 69 (1980) 413–434.
[30] T. Hiyama, B. Ke, Biochim. Biophys. Acta 257 (1978) 160–171.
[31] D.I. Arnon, Plant Physiol. 24 (1949) 1–15.
[32] J.H. Nugent, B.L. Moller, M.C.W. Evans, Biochim. Biophys. Acta 634 (1981) 249–255.
[33] M.C.W. Evans, S. Purton, V. Pate, D. Wright, P. Heathcote, S.E.J. Rigby, Photosynth. Res. 61 (1999) 33–42.
[34] Y.S. Jung, I.R. Vassiliev, J. Yu, L. McIntosh, J.H. Golbeck, J. Biol. Chem. 272 (1997) 8040–8049.